

Hen Process in Effective Field Theory

Young-Ho Song^(a) and Tae-Sun Park^(b)

(a) Department of Physics, Seoul National University, Seoul 151-742, Korea and

(b) School of Physics, Korea Institute for Advanced Study, Seoul 130-012, Korea

(Dated: December 10, 2018)

An effective field theory technique that combines the standard nuclear physics approach and chiral perturbation theory is applied to the *hen* process, ${}^3\text{He}+n \rightarrow {}^4\text{He}+\gamma$. For the initial and final nuclear states, high-precision wave functions are generated via the variational Monte Carlo method using the Argonne v_{14} potential and Urbana VIII trinucleon interactions, while the relevant transition operators are calculated up to $\mathcal{O}(Q^4)$ in HB χ PT. The imposition of the renormalization condition that the magnetic moments of ${}^3\text{He}$ and ${}^3\text{H}$ be reproduced allows us to carry out a parameter-free calculation of the *hen* cross section. The result, $\sigma = (60 \pm 3 \pm 1) \mu\text{b}$, is in reasonable agreement with the experimental values, $(54 \pm 6) \mu\text{b}$ and $(55 \pm 3) \mu\text{b}$. This agreement demonstrates the validity of the calculational method previously used for estimating the reaction rate of the solar *hep* process.

One of the important advantages of using effective field theory (EFT) in nuclear physics is that it leads to well-controlled predictions for nuclear observables over which the conventional model approaches have little or no control. One such case is the *hep* process ${}^3\text{He}+p \rightarrow {}^4\text{He}+\nu_e+e^+$, which can be potentially important for solar neutrino physics and non-standard physics in the neutron sector. In a recent paper, Park *et al.* [1] have developed an EFT approach, to be referred to as “MEEFT” [2], and succeeded in making a totally parameter-free calculation of the *hep* cross section. In MEEFT, the relevant transition operators are systematically derived using chiral perturbation theory, while the initial and final nuclear wave functions are generated using the standard nuclear physics approach (SNPA). Here SNPA refers to an approach in which the wave functions of light nuclei (mass number A) are obtained by solving exactly the A -body Schrödinger equation with a Hamiltonian that contains a high-precision phenomenological potential. With the use of MEEFT, Park *et al.* arrived at a prediction of the *hep* S -factor with $\sim 15\%$ accuracy. Given the fact that the predicted values of the *hep* S -factor ranged over two orders of magnitude in the past, the result obtained in [1] could be considered a remarkable feat. It is to be noted, however, that the $\sim 15\%$ uncertainty associated with the *hep* S -factor (although acceptable on its own merit) is strikingly larger than the uncertainty associated with the S -factor for the *pp* fusion process, the latter estimated to be less than 0.5% [1]. There are two plausible causes for such a “large” uncertainty in the *hep* calculation. First, since the calculation in [1] relies entirely on the information provided by the two-body and three-body observables, it may miss part of the dynamics which is intrinsically four-body in nature. Secondly, symmetry mismatch between the initial and final states of the *hep* process, a feature that is absent in the two- and three-body systems, induces a strong suppression of the otherwise dominant single-particle contribution, resulting in an enhancement of higher-order corrections, perhaps including four-body interactions.

The purpose of this Letter is to test the reliability of MEEFT used to compute the *hep* process by applying

the same method to the *hen* process

$${}^3\text{He} + n \rightarrow {}^4\text{He} + \gamma \quad (1)$$

at threshold; *hen* is a four-body process that has close similarity to *hep* in that the pseudo-orthogonality of the initial and final wave functions strongly suppresses the leading-order one-body contribution. In fact, the degree of suppression for *hen* is such that the exchange current “corrections” become dominant terms. Meanwhile, since the experimental value of the threshold *hen* process is known with reasonable accuracy: $\sigma_{exp} = (54 \pm 6) \mu\text{b}$ [3] and $\sigma_{exp} = (55 \pm 3) \mu\text{b}$ [4], *hen* provides a good testing ground for the validity of MEEFT. It is to be noted that these experimental values have never been explained satisfactorily before. We remark, in particular, that very elaborate SNPA calculations by Carlson *et al.* [5] and by Schiavilla *et al.* [6] give $\sigma = 112 \mu\text{b}$ and $\sigma = 86 \mu\text{b}$, respectively. It has been noted that σ is extremely sensitive to the ${}^3\text{He}+n$ scattering length, a_n ; the use of the updated value, $a_n^{\text{exp}} = 3.278(53) \text{ fm}$ [7], makes the calculated σ even larger. In view of the high quality of the wave functions used in these calculation, it is very probable that the problem lies in the many-body currents used. This observation makes the use of MEEFT for *hen* all the more interesting.

Our parameter-free calculation based on MEEFT gives for the threshold *hen* cross section

$$\sigma = (60.1 \pm 3.2 \pm 1.0) \mu\text{b}, \quad (2)$$

which agrees with the above-quoted experimental values.

The strategy of MEEFT, explained in [1, 8], is close in spirit to Weinberg’s original scheme [9] based on the chiral expansion of “irreducible terms”. MEEFT has been used with great success to describe the highly suppressed isoscalar amplitude pertaining to the $n+p \rightarrow d+\gamma$ process [10, 11] and many weak processes (for a recent review, see Ref. [12]). In MEEFT, the relevant current operators are derived systematically by applying heavy-baryon chiral perturbation theory (HB χ PT) up to a specified order. The nuclear matrix elements are then evaluated by sandwiching these current operators between

the high-precision wave functions obtained in SNPA. In EFT, short-distance physics is represented as contact counter-terms, and the coefficients of these terms, called the low-energy constants (LECs) are determined by requiring that a selected set of experimental data be reproduced. This renormalization procedure is expected to remove to a large extent the model-dependence of the short-range behavior of the adopted phenomenological wave functions, and this feature is very important for making model-independent predictions. We should note here that the strategy employed here is closely related to that used for the universal V_{low-k} in the recent renormalization-group approach to nuclear interactions [13].

The total cross section of the *hen* reaction reads

$$\sigma = \frac{2\alpha\omega}{v_n} \frac{1}{4} \sum_{M=-1}^1 |{}^4\text{He}|\mathbf{j}_T(\mathbf{q})|n+{}^3\text{He}; 1M|^2, \quad (3)$$

where α is the fine structure constant, (ω, \mathbf{q}) is the four-momentum of the outgoing photon with $|\mathbf{q}| = \omega \simeq 20.521$ MeV, v_n is the velocity of the incident thermal neutron, M is the spin quantum number of the initial system, and \mathbf{j}_T is the electromagnetic (EM) current operator transverse to the photon direction. As the process is isotropic at threshold, we can choose $\hat{\mathbf{q}} = \hat{\mathbf{z}}$.

The formalism employed here is essentially the same as in the *hep* process, so we refer to Ref.[1] whenever appropriate. We obtain the EM current using HB χ PT, which contains the nucleons and pions as explicit degrees of freedom, with all the other massive fields integrated out. In HB χ PT, operators carry a typical momentum scale of the process and/or the pion mass, which is regarded as small compared to the chiral scale $\Lambda_\chi \sim 4\pi f_\pi \sim m_N \sim 1$ GeV, where $f_\pi \simeq 93$ MeV is the pion decay constant and $m_N \simeq 939$ MeV the nucleon mass. The leading space-components of the EM currents are of order of Q , and hence we refer to terms of order Q^{n+1} as $N^n\text{LO}$. In this paper, we shall limit ourselves up to $N^3\text{LO}$ or $\mathcal{O}(Q^4)$. It is important to take into account the kinematical suppression of the time component of the nucleon four-momentum and the smallness of the photon energy/momentum. For simplicity, we count the time component of the nucleon four-momentum q_0 and $|\mathbf{q}|$ as Q^2 order rather than Q . *It is important to emphasize that, up to $N^3\text{LO}$, three-body and four-body current operators do not appear.* This means that the nuclear systems with $A = 2, 3$ and 4 can all be described by the *same* current operators up to this order.

The leading order one-body (1B) currents are given by

$$\mathbf{J}_i = e^{-i\mathbf{q}\cdot\mathbf{r}_i} \left[\frac{(1+\tau_i^z)}{2m_N} \bar{\mathbf{p}}_i + \frac{(\mu_S + \mu_V \tau_i^z)}{4m_N} i\mathbf{q} \times \boldsymbol{\sigma}_i \right] \quad (4)$$

where, $\bar{\mathbf{p}} \equiv \frac{1}{2}(i \overleftrightarrow{\nabla} - i \overrightarrow{\nabla})$ acts only on the wave function. Relativistic corrections to the 1B currents are also included in the calculation. It should be noted

that the two-body (2B) currents in momentum space are valid only up to a certain cutoff Λ . This implies that the currents should be appropriately regulated. This is the key point in our approach. This cutoff defines the energy/momentum scale of EFT below which reside the chosen explicit degrees of freedom. We use a Gaussian regulator in performing the Fourier transformation from momentum to coordinate space. All the 2B currents can be written in the form of $\mathbf{J}_{12}(\mathbf{r}_1, \mathbf{r}_2) = e^{-i\mathbf{q}\cdot(\mathbf{r}_1+\mathbf{r}_2)/2} \mathbf{j}_{12}(\mathbf{r}_1 - \mathbf{r}_2)$. The $N^1\text{LO}$ correction is due to the *soft*-one-pion-exchange,

$$\begin{aligned} \mathbf{j}_{12}^{1\pi}(\mathbf{r}) = & -\frac{g_A^2 m_\pi^2}{12f_\pi^2} \boldsymbol{\tau}_\times^z \mathbf{r} [\boldsymbol{\sigma}_1 \cdot \boldsymbol{\sigma}_2 \bar{y}_{0\Lambda}^\pi(\mathbf{r}) + S_{12} y_{2\Lambda}^\pi(\mathbf{r})] \\ & + i \frac{g_A^2}{8f_\pi^2} \mathbf{q} \times [\hat{T}_S^{(\times)} (\frac{2}{3} y_{1\Lambda}^\pi(\mathbf{r}) - y_{0\Lambda}^\pi(\mathbf{r})) - \hat{T}_T^{(\times)} y_{1\Lambda}^\pi(\mathbf{r})], \end{aligned} \quad (5)$$

where $g_A = 1.2601$, $S_{12} = 3\boldsymbol{\sigma}_1 \cdot \hat{\mathbf{r}} \boldsymbol{\sigma}_2 \cdot \hat{\mathbf{r}} - \boldsymbol{\sigma}_1 \cdot \boldsymbol{\sigma}_2$; we have also defined $\hat{T}_{S,12}^{(\odot)} \equiv \boldsymbol{\tau}_\odot^z \boldsymbol{\sigma}_\odot$ and $\hat{T}_{T,12}^{(\odot)} \equiv \boldsymbol{\tau}_\odot^z [\hat{\mathbf{r}} \hat{\mathbf{r}} \cdot \boldsymbol{\sigma}_\odot - \frac{1}{3} \boldsymbol{\sigma}_\odot]$, $\boldsymbol{\tau}_\odot = \boldsymbol{\tau}_1 \odot \boldsymbol{\tau}_2$, $\boldsymbol{\sigma}_\odot = \boldsymbol{\sigma}_1 \odot \boldsymbol{\sigma}_2$, $\odot = \pm, \times$. The explicit forms of the regulated Yukawa functions are given in Ref.[1].

There are no corrections at $N^2\text{LO}$. At $N^3\text{LO}$, there occur vertex corrections to the one-pion exchange $j^{1\pi C}$, the two-pion-exchanges $j^{2\pi}$, and the contact counter-term contributions j^{CT} . The $j^{1\pi C}$ investigated in detail in Ref. [10, 11] reads

$$\begin{aligned} \mathbf{j}_{12}^{1\pi C} = & i\mathbf{q} \times \left\{ -\frac{g_A^2}{8f_\pi^2} (\bar{c}_\omega + \bar{c}_\Delta) [(\hat{T}_S^{(+)} + \hat{T}_S^{(-)}) \frac{\bar{y}_{0\Lambda}^\pi}{3} \right. \\ & \left. + (\hat{T}_T^{(+)} + \hat{T}_T^{(-)}) y_{2\Lambda}^\pi] - \frac{g_A^2}{16f_\pi^2} \bar{c}_\Delta \hat{T}_T^{(\times)} y_{2\Lambda}^\pi \right. \\ & \left. + \frac{1}{16f_\pi^2} \bar{N}_{WZ} \boldsymbol{\tau}_1 \cdot \boldsymbol{\tau}_2 [\boldsymbol{\sigma}_+ \bar{y}_{0\Lambda}^\pi + (3\hat{\mathbf{r}} \cdot \boldsymbol{\sigma}_+ - \boldsymbol{\sigma}_+) y_{2\Lambda}^\pi] \right\}, \end{aligned} \quad (6)$$

where $\bar{c}_\omega \simeq 0.1021$, $\bar{c}_\Delta \simeq 0.1667$, and $\bar{N}_{WZ} \simeq 0.02395$. Although $j^{1\pi C}$ contains the so-called ‘‘fixed terms’’ needed to ensure Lorentz covariance, we neglect them here since they are expected to be small. The two-pion-exchange diagrams, except for the box-diagrams, can be found in ref.[10]. Adding the box-diagram contributions and subtracting the reducible iterated one-pion-exchange part, we obtain

$$\begin{aligned} \mathbf{j}_{12}^{2\pi} = & -\frac{1}{128\pi^2 f_\pi^4} \left\{ (\tau_1 \times \tau_2)^z \hat{\mathbf{r}} \frac{d}{dr} L_0 \right. \\ & \left. - i\mathbf{q} \times \left[(\hat{T}_S^{(+)} - \hat{T}_S^{(-)}) L_S + (\hat{T}_T^{(+)} - \hat{T}_T^{(-)}) L_T \right] \right\} \end{aligned} \quad (7)$$

with

$$\begin{aligned} L_0 = & 2K_2 + g_A^2(16K_2 - 2K_1 - 2K_0) \\ & - g_A^4(16K_2 + 5K_1 + 5K_0) + g_A^4 \frac{d}{dr}(rK_1), \\ L_S = & \frac{g_A^2}{3} r \frac{d}{dr} K_0 + \frac{g_A^4}{3} [4K_1 - 2K_0 + r \frac{d}{dr}(K_0 + 2K_1)], \\ L_T = & -\frac{g_A^2}{2} r \frac{d}{dr} K_0 + \frac{g_A^4}{3} [4K_T - r \frac{d}{dr}(K_0 + 2K_1)]. \end{aligned} \quad (8)$$

The loop functions K' s are defined in Ref. [1, 10]. Finally there are contact contributions of the form

$$\mathbf{j}_{12}^{\text{CT}} = \frac{i}{2m_p} \mathbf{q} \times [g_{4S}(\boldsymbol{\sigma}_1 + \boldsymbol{\sigma}_2) + g_{4V} T_S^{(\times)}] \delta_\Lambda^{(3)}(\mathbf{r}), \quad (9)$$

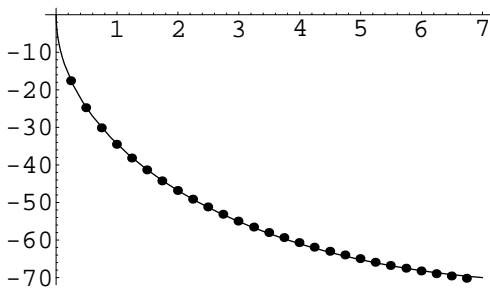


FIG. 1: The ${}^3\text{He} + n$ S-wave phase shift in degrees as a function of the center-of-mass energy in MeV. The solid line gives our results obtained with the Woods-Saxon potential, while the full dots represent the experimental data obtained from an R -matrix analysis [14].

where $g_{4S} = m_p g_4$ and $g_{4V} = -m_p(G_A^R + \frac{1}{4}E_T^{V,R})$, m_p is the proton mass; g_4 , G_A^R and $E_T^{V,R}$ are the coefficients of the counter-terms introduced in [10, 11]. A highly noteworthy point is that, although there are many possible counter-terms, only two linear combinations of them are independent for the M1 transition. This reduction of the effective number of counter terms is due to the Fermi-Dirac statistics; a similar reduction has been noted for hep [1], where only one linear combination of LECs needs to be retained.

As the cutoff Λ has a physical meaning, its choice is not arbitrary. Obviously, Λ greater than Λ_χ should be excluded. Furthermore, Λ should not be larger than the mass of the vector mesons that have been integrated out; thus, $\Lambda \lesssim 800$ MeV. Meanwhile, since the pion is an explicit degree of freedom in our scheme, Λ should be much larger than the pion mass in order to ensure that all pertinent low-energy contributions are properly included. In the present work, we adopt $\Lambda = 500, 600$ and 800 MeV as representative values.

We use realistic variational Monte-Carlo wave functions obtained for the Argonne v14 two-nucleon interaction and the Urbana VIII trinucleon interactions; these are the potentials used in the previous SNPA calculation[5]. The asymptotic behavior of the ${}^3\text{He} + n$ system has been taken into account by means of the Woods-Saxon (WS) potential, $V_{WS}(r) = V_0(1 + e^{(r-R_0)/d_0})^{-1}$. We can determine the parameters in the WS potential so as to reproduce the experimental data for the scattering length [7] and the low-energy phase shifts [14]; the results are $V_0 = 8.63637$ MeV, $R_0 = 4.14371$ fm and $d_0 = 0.8$ fm. It should be pointed out [5] that a small difference a_n can affect the hen cross section significantly. For this reason the experimental data are directly encoded into theory. The resulting phase shifts are shown in figure 1. The precise measurement of the ${}^3\text{He} + n$ scattering length enables us to limit the uncertainty associated with the scattering length to $\lesssim 1\%$ in the matrix elements. The nuclear matrix elements of the currents are evaluated by taking 1

TABLE I: The magnetic moment of ${}^3\text{H}$ and ${}^3\text{He}$ (in units of μ_N), and the hen matrix elements $\langle j \rangle_{hen}$ (in units of 10^{-3} fm $^{3/2}$), calculated for $\Lambda = 600$ MeV. The numbers in the parentheses represent Monte-Carlo statistical errors.

	$\mu({}^3\text{H})$	$\mu({}^3\text{He})$	$\langle j \rangle_{hen}$
1B	2.6068(1)	-1.7839(1)	-1.76(1)
2B($1\pi + 1\pi C$)	0.2676(3)	-0.2975(3)	5.89(3)
2B(2π)	0.0334(1)	-0.0334(1)	0.90(1)
2B(CT)	0.0710(3)	-0.0128(3)	0.35(1)
2B(total)	0.3721(1)	-0.3437(1)	7.14(3)
1B+2B	2.9789	-2.1276	5.39(3)

million samplings in the Metropolis algorithm.

For each value of Λ , we adjust the values of the two independent LECs (denoted by g_{4s} and g_{4v}) so as to reproduce the experimental values of the ${}^3\text{H}$ and ${}^3\text{He}$ magnetic moments. The results are $\{g_{4s}, g_{4v}\} = \{1.079(9), 2.029(6)\}$, $\{1.277(12), 0.981(7)\}$ and $\{1.856(22), -0.235(12)\}$ for $\Lambda = 500, 600$ and 800 MeV, respectively. Once the values of $g_{4s,4v}$ are fixed, we can predict the M1 transition amplitude for hen without any unknown parameters.

In Table I, we list the contributions of various terms to the magnetic moment of ${}^3\text{H}$ and ${}^3\text{He}$ and the hen matrix elements $\langle j \rangle_{hen} \equiv \frac{1}{2} \langle {}^4\text{He} | (j_x - ij_y) | n + {}^3\text{He}; 11 \rangle$, calculated for $\Lambda = 600$ MeV. The row labelled “2B($1\pi + 1\pi C$)” gives contributions from eqs.(5,6), “2B(2π)” from eq.(7), and “2B(CT)” from eq.(9); “2B(total)” represents the sum of all these contributions. As mentioned, the 1B contribution is *strongly* suppressed by the pseudo-orthogonality of the wave functions, and as a result the matrix element is dominated by the $\langle 2B \rangle$. Furthermore, since the 2B and 1B contributions have opposite signs, there is destructive interference between them, which, as in the hep case, makes it a more challenging task to obtain an accurate estimate of the cross section. A highly significant feature is that the ratio of the 2B to 1B contribution for hen is about -4 , which is much larger in magnitude than the corresponding ratio hep , which is about -0.6 . This large difference can be understood by recalling the “chiral filter mechanism” argument [15] according to which the $N^1\text{LO}$ contribution is non-vanishing for hen , while the 2B correction in hep only starts at $N^3\text{LO}$. It is remarkable that, despite this difference, exactly the same MEEFT strategy works for both hep and hen .

The cutoff dependence of the matrix elements and the corresponding cross section are shown in Table II. We remark that the 1B matrix element has no cutoff dependence. It is noteworthy that the cutoff dependence seen in the hen case is quite similar to that seen in the hep case. While the individual contributions of the contact and non-contact terms vary strongly as functions of Λ , their sum shows a greatly reduced Λ -dependence. This can be interpreted as a manifestation (albeit approximate) of the renormalization group invariance of

TABLE II: The cutoff dependence of the matrix elements (in $10^{-3} \text{ fm}^{3/2}$) and the corresponding total cross sections for $\Lambda = 500, 600$ and 800 MeV .

$\Lambda(\text{MeV})$	500	600	800
1B	-1.76(1)	-1.76(1)	-1.76(1)
2B(non-contact terms)	5.24(2)	6.79(3)	8.31(3)
2B(contact terms)	1.80(1)	0.35(1)	-0.99(1)
2B total	7.04(2)	7.14(3)	7.32(6)
1B+2B	5.29(2)	5.39(3)	5.57(6)
$\sigma(\mu b)$	56.9(3)	59.2(5)	63.2(10)

physical observables. The smallness of the cutoff dependence, $\sim 3\%$, seen in Table II indirectly indicates that our MEEFT scheme allows us to control short-range dynamics to a satisfactory degree. The remaining small cutoff dependence may be attributed to the contributions of terms ignored in this calculation, *e.g.*, the “fixed” terms, n -body currents for $n > 2$, other higher chiral order terms, etc. Our final value for the threshold *hen* cross section is $\sigma = (60.1 \pm 3.2 \pm 1.0) \mu b$, where the first error comes from the cutoff dependence and the second from the statistical errors. Errors arising from the uncertainties in the n - ^3He scattering length are estimated to be $\sim 1\%$ in the matrix element.

We have already mentioned that the existing SNPA calculations for *hen* cannot explain σ_{exp} . A comment is in order on this point since, for all the other cases so far studied in both SNPA and MEEFT (*pp* fusion, *hep*, $\nu - d$ scattering, radiative *np*-capture *etc*), the numerical results exhibit a close resemblance (except that the MEEFT results come with systematic error estimates.) As mentioned, one of the most important ingredients of MEEFT is a “renormalization” procedure in which the relevant unknown LECs are fixed using the experimental values of observables in neighboring nuclei. A similar procedure has been done in the SNPA calculations of the above-quoted cases. However, the existing SNPA calculation of *hen* [5, 6], lacks this “renormalization”, and this

explains why the “existing” SNPA calculation of σ_{hen} disagrees with the experimental data.

To summarize, we have carried out an MEEFT calculation for *hen* up to $N^3\text{LO}$ and provided the first theoretical explanation of the experimental value of the *hen* cross section, σ . Because of the drastic suppression of the leading-order one-body term, which makes the sub-leading exchange-current a dominant term, and a significant cancellation between these two contributions, an *unnatural* amplification of the cutoff dependence occurs, as in the *hep* case. Despite this accidental “fine-tuning” situation, we have shown that MEEFT allows us to make a parameter-free estimation of σ_{hen} with accuracy better than $\sim 10\%$. The successful application of MEEFT to *hen* renders strong support for the results of our previous MEEFT calculation for *hep*; furthermore, it demonstrates the basic soundness of the MEEFT strategy in general. The present treatment is open to several improvements such as going to the next order in chiral perturbation, using more accurate SNPA wave functions, a more stringent control of mismatch in the chiral counting between SNPA and a formally accurate chiral expansion that enters in the currents, a better understanding of the role that the counter terms play in the renormalization group property, etc. It is reasonable, however, to expect that the effects of these improvements are essentially accommodated in the above-quoted error estimate based on the cutoff dependence. A robust estimation of the *hep* S-factor has been a long-standing challenging problem in nuclear physics [16]. We believe that our MEEFT calculation of *hep* and *hen* have solved this problem to a satisfactory degree. Short of doing a fully formally consistent EFT calculation, which is at present out of our reach, MEEFT seems the best one could do at moment.

We would like to acknowledge invaluable discussions with, and support from, Professors K. Kubodera, D.-P. Min and M. Rho with whom this work was initiated. The work of TSP was supported by Korea Research Foundation Grant(KRF-2001-050-D00007).

-
- [1] T.-S. Park *et al.*, Phys. Rev. **C67**, 055206 (2003), nucl-th/0208055.
 - [2] G.E. Brown and M. Rho, nucl-th/0305089, to appear in Phys. Rep.
 - [3] F.L.H. Wolfs *et al.*, Phys. Rev. Lett. **63**, 2721 (1989).
 - [4] R. Wervelman *et al.*, Nucl. Phys. **A526**, 265 (1991).
 - [5] J. Carlson, D.O. Riska, R. Schiavilla and R.B. Wiringa, Phys. Rev. **C42**, 830 (1990).
 - [6] R. Schiavilla, R.B. Wiringa, V.R. Pandharipande, and J. Carlson, Phys. Rev. **C**, **45** 2628 (1992).
 - [7] O. Zimmer *et al.*, EJPdirect **A1**, 1 (2002).
 - [8] T.-S. Park, K. Kubodera, D.-P. Min, and M. Rho, Nucl. Phys. **A684**, 101 (2001).
 - [9] S. Weinberg, Phys. Lett. **B251**, 288 (1990); Nucl. Phys. **B363**, 3 (1991); Phys. Lett. **B295**, 114 (1992).
 - [10] T.-S. Park, D.-P. Min and M. Rho, Phys. Rev. Lett. **74**, 4153 (1995); Nucl. Phys. **A596**, 515 (1996).
 - [11] T.-S. Park, K. Kubodera, D.-P. Min, and M. Rho, Phys. Lett. **B472**, 232 (2000).
 - [12] K. Kubodera, nucl-th/0308055.
 - [13] S.K. Bogner, T.T.S. Kuo and A. Schwenk, Phys. Rep. **386**, 1 (2003).
 - [14] H.M. Fofmann and G.M. Hale, Nucl. Phys. **A613**, 69 (1997).
 - [15] K. Kubodera, J. Delorme and M. Rho, Phys. Rev. Lett. **40**, 755 (1978); M. Rho, Phys. Rev. Lett. **66**, 1275 (1991).
 - [16] J.N. Bahcall, Phys. Rep. **333**, 47 (2000), and references therein.